

## $\beta$ -Ga<sub>2</sub>O<sub>3</sub> nanorods crossing perpendicularly each other on MgO (100) substrate

SHIGEMI KOHIKI, KIMIHIRO YASUI, KYOKO HORI, MASAHIRO FUKUTA, WATARU YAMAUCHI, HIROKAZU SHIMOOKA

Department of Materials Science, Kyushu Institute of Technology, 1-1 Sensui, Tobata, Kitakyushu 804-8550, Japan

TOETSU SHISHIDO, MASAOKI OKU

Institute for Materials Research, Tohoku University, 2-1-1 Katahira, Aoba, Sendai 980-8577, Japan

MASANORI MITOME, YOSHIO BANDO

Advanced Materials Laboratory, National Institute for Materials Science, 1-1 Namiki, Tsukuba, Ibaraki 305-0044, Japan

Growth and characterization of nanowires and nanorods of wide bandgap ( $E_g$ ) compounds [1–14] have attracted much attention due to significant potential of such one-dimensional materials for optoelectronic applications [15, 16]. It was reported that transparent  $\beta$ -Ga<sub>2</sub>O<sub>3</sub> ( $E_g \approx 4.9$  eV) [17] has potential application in optoelectronics [18], and nanometer-scale Ga<sub>2</sub>O<sub>3</sub> exhibits particular optical and electrical properties [19].  $\beta$ -Ga<sub>2</sub>O<sub>3</sub> is intrinsically an insulator useful for all gallium-based semiconductors but becomes an  $n$ -type semiconductor when synthesized under reducing conditions. Recent requirements for improved transparency and higher conductivity have led to explore new transparent conducting oxides available in a variety of devices including low-power driven flat-panel displays and high-efficiency solar energy-conversion devices. One-dimensionally structured  $\beta$ -Ga<sub>2</sub>O<sub>3</sub> is expected to provide attractive characteristics for its practical applications as well as for fabricating nanodevices with novel properties.

Growth of the nanorods by vapor phase transport method was carried out in a horizontal furnace. A  $\beta$ -Ga<sub>2</sub>O<sub>3</sub> single crystal<sup>20</sup> was pulverized and loaded in an alumina boat. The boat and the MgO substrate coated with a thin Au layer were transferred to the places of 1200 and 640 °C in an alumina tube of the furnace, respectively. In a typical run, the Au layer was evaporated in a vacuum ( $2 \times 10^{-5}$  Torr) on the substrate, and the layer consisted of Au nanospheres with about several tens of nanometers in diameter. First, the tube was pumped out by a rotary pump, and then it was heated up to 1200 °C at the rate of 10 °C/min in a flow of mixed gas (95% N<sub>2</sub> and 5% H<sub>2</sub>). The substrate placed downstream of the gas flow. At 1200 °C, the temperature was kept constant for 180 min. After cooling down to room temperature, a white layer was found on the substrate. The white layer was characterized by using a JEOL JSM-6320F scanning electron microscope (SEM), a JEOL JEM-3100FEF transmission electron microscope (TEM) operated at 300 kV, an energy dispersive X-ray spectrometer (EDX) equipped to the microscope, and a Rigaku CN2031 X-ray diffrac-

tometer (XD) with Cu K $\alpha$  radiation. Optical emission spectrum in ultraviolet-visible region was measured under 240 nm-line irradiation using a JASCO V-560 spectrometer.

As shown in Fig. 1a, a low magnification SEM image revealed that the white layer consists of a large quantity of conical shaped nanorods crossing perpendicularly each other on the substrate. Most of the nanorods were straight, and typical lengths were in the range of several to ten micrometers. In a high magnification image of Fig. 1b, we see that the diameter was up to one micrometer around the root of the conical nanorods but decreased to few hundreds nanometers on approaching the tip. Such typical values in the length and diameter result in a very large aspect ratio for the nanorods, which are in the range of approximately 10–50. As seen in Fig. 1b, each nanorods had a nanosphere with diameters of few hundreds nanometers at the tip. The diameter

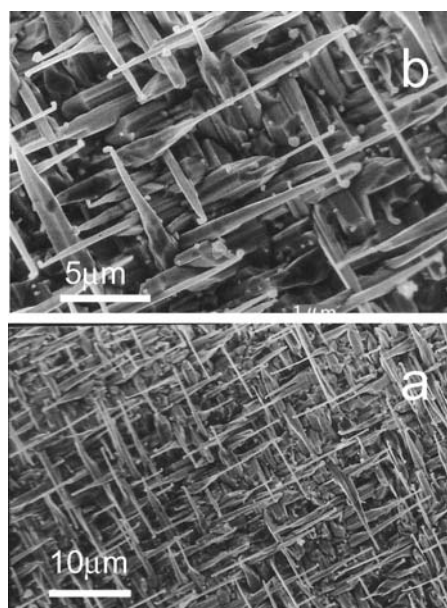


Figure 1 SEM images with relatively low (a) and high (b) magnification of  $\beta$ -Ga<sub>2</sub>O<sub>3</sub> nanorods grown on MgO (100) substrate.

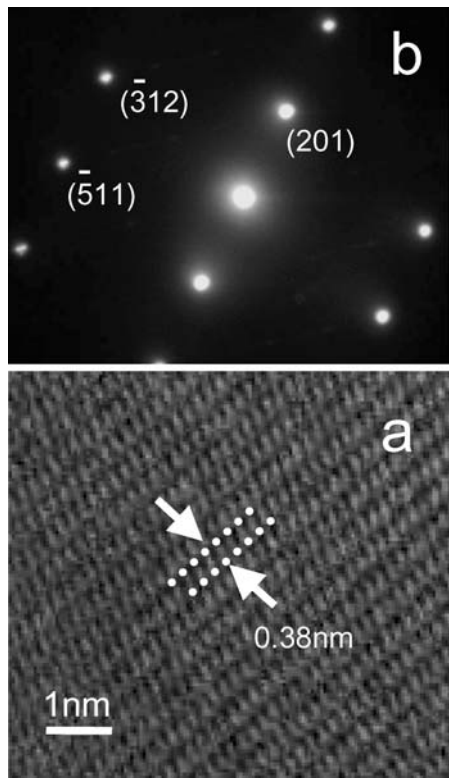


Figure 2 Lattice image (a) and electron diffraction pattern (b) of a  $\beta$ - $\text{Ga}_2\text{O}_3$  nanorod by TEM.

of the nanosphere looks larger than that of the nanorod nearby the tip.

The crystal structure of the nanorods was characterized by TEM and XD. Elemental analysis of individual nanorod was performed using EDX equipped to the TEM. For TEM observation, the nanorods were scraped away from the substrate surface and dispersed in ethanol, and then the ethanol solution was sprayed onto a copper grid coated carbon film. A structure image of a nanorod with clear lattice fringes of  $\beta$ - $\text{Ga}_2\text{O}_3$  was obtained, as shown in Fig. 2a. The periodicity of 0.38 nm between the arrowheads corresponds to distance between the (201) planes of  $\beta$ - $\text{Ga}_2\text{O}_3$  crystal. No microtwins, stacking faults, and other planer defects were found in some nanorods. An electron diffraction pattern of the nanorod shown in Fig. 2b can be indexed to the monoclinic  $\beta$ - $\text{Ga}_2\text{O}_3$  (JCPDS 11-370). Some Miller indices were labeled on the spots. All spots can be attributed to the structure with lattice constants of  $a = 1.223$  nm,  $b = 0.304$  nm,  $c = 0.580$  nm, and  $\beta = 103.7^\circ$ , and with the space group of  $C2/m$ . The nanorods gave an XD pattern mirroring epitaxial growth of  $\beta$ - $\text{Ga}_2\text{O}_3$  crystal on the substrate, as shown in Fig. 3. The (400) plane of the  $\beta$ - $\text{Ga}_2\text{O}_3$  nanorods is parallel to the (100) plane of the MgO substrate. The EDX analysis indicated that the nanorods are composed of Ga and O. The Ga/O ratio of the nanorods was consistent with that of single crystalline  $\beta$ - $\text{Ga}_2\text{O}_3$  [21]. Emission spectrum was measured to examine the optical property of the  $\beta$ - $\text{Ga}_2\text{O}_3$  nanorods. While the  $\beta$ - $\text{Ga}_2\text{O}_3$  crystalline powders used as raw material in this experiment exhibited blue-emission centered at 400 nm under illumination of 240 nm-light, the  $\beta$ - $\text{Ga}_2\text{O}_3$  nanorods showed no emission due to the defects such

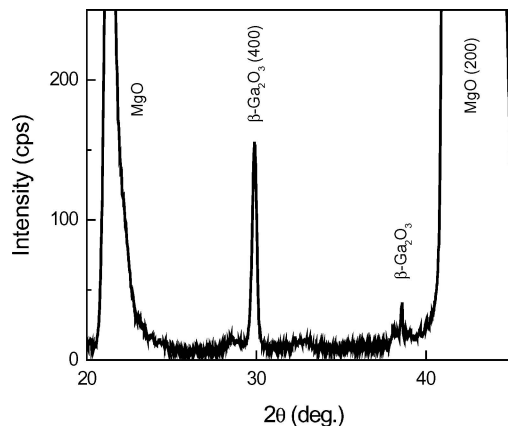


Figure 3 XD pattern of the  $\beta$ - $\text{Ga}_2\text{O}_3$  nanorods grown on MgO (100) substrate. The peak at  $2\theta \approx 30^\circ$  can be assigned to reflection from the (400) plane of  $\beta$ - $\text{Ga}_2\text{O}_3$ . At  $2\theta \approx 39^\circ$ , we see a weak signal ascribable to reflection from the (311) plane of  $\beta$ - $\text{Ga}_2\text{O}_3$ . Peaks at  $2\theta \approx 21^\circ$  and  $\approx 42^\circ$  are due to the MgO substrate. Most of the nanorods grew epitaxially on the substrate. The  $\beta$ - $\text{Ga}_2\text{O}_3$  (400) plane was parallel to the MgO (100) plane.

as oxygen vacancies and Ga-O vacancy pairs under such illumination. The optical emission spectrum confirmed a high-quality crystal growth of the nanorods. These are in good agreement with the result of structural characterization.

There are two models for the growth of conventional crystal nanorods, the screw dislocation and vapor-liquid-solid (VLS) process. As shown in Fig. 1b, each elongated nanorods terminates in a nanosphere at the tip. EDX analysis indicated that the nanosphere on the tip consisted of Au but the stem was constructed with  $\text{Ga}_2\text{O}_3$ . The Au nanosphere looks larger than the  $\beta$ - $\text{Ga}_2\text{O}_3$  nanorod nearby the tip. In our TEM observation, the surfaces of the  $\beta$ - $\text{Ga}_2\text{O}_3$  nanorods were clean and there was no sheathe of amorphous phase. These results suggest that the growth of the nanorods may be dominated by the VLS process [22]. In VLS growth process, a metal particle is located at the growth front of the rod and acts as the catalytic active site. The solidified spherical droplets at the tips of the nanorods are commonly considered to be the evidence for the operation of the VLS mechanism, which is in agreement with our results.

Here, we have reported growth of  $\beta$ - $\text{Ga}_2\text{O}_3$  nanorods capped with Au nanosphere. The conical nanorods consisting of monoclinic  $\beta$ - $\text{Ga}_2\text{O}_3$  single crystals crossed perpendicularly each other on the (100) plane of the MgO substrate. Typical lengths of the nanorods were in the range of several to ten micrometers. Diameters were up to one micrometer around the root of the conical nanorods and decreased to few hundreds nanometers with approaching to the tip. The Au nanospheres with diameters of few hundreds nanometers placed at the tip. The Au nanosphere played a crucial role in the growth of  $\beta$ - $\text{Ga}_2\text{O}_3$  nanorods based on the VLS mechanism.

### Acknowledgment

A part of this work performed under the inter-university research program of Laboratory for Advanced Materials, the Institute of Materials Research, Tohoku

University. A part of this work was also supported by “Nanotechnology Support Project” of the Ministry of Education, Culture, Sports, Science and Technology (MEXT), Japan.

## References

1. H. Z. ZHANG, Y. C. KONG, Y. Z. WANG, X. DU, Z. G. BAI, J. J. WANG, D. P. YU, Y. DING, Q. L. HANG and S. Q. FENG, *Solid State Commun.* **109** (1999) 677.
2. Y. C. CHOI, W. S. KIM, Y. S. PARK, S. M. LEE, D. J. BAE, Y. H. LEE, G. S. PARK, W. B. CHOI, N. S. LEE and J. M. KIM, *Adv. Mater.* **12** (2000) 746.
3. J. Y. LI, Z. Y. QIAO, X. L. CHEN, L. CHEN, Y. G. CAO, M. HE, H. LI, Z. M. CAO and Z. ZHANG, *J. Alloys Composts.* **306** (2000) 300.
4. W. Q. HAN, P. KOHLER-REDLICH, F. ERNST and M. RUEHLE, *Solid State Commun.* **115** (2000) 527.
5. C. H. LIANG, G. W. MENG, G. Z. WANG and L. D. ZHANG, *Appl. Phys. Lett.* **78** (2001) 3202.
6. D. P. YU, J. L. BUBENDORFF, J. F. ZHOU, Y. LEPRINCE-WANG and M. TROYON, *Solid State Commun.* **124** (2002) 417.
7. G. GUNDIAH, A. GOVINDARAJ and C. N. R. RAO, *Chem. Phys. Lett.* **351** (2002) 189.
8. J. ZHANG and F. JIANG, *Chem. Phys.* **289** (2003) 243.
9. P. YANG and C. M. LIEBER, *Science* **273** (1996) 1836.
10. Z. L. WANG, R. P. GAO, J. L. GOLE and J. D. STOUT, *Adv. Mater.* **12** (2000) 1938.
11. C. H. LIANG, C. W. MENG, Y. LEI, F. PHILLIP and L. D. ZHANG, *ibid.* **13** (2001) 1330.
12. Z. G. BAI, D. P. YU, H. Z. ZHANG, Y. DING, X. Z. GAI, Q. L. HANG, G. C. XIONG and S. Q. FENG, *Chem. Phys. Lett.* **303** (1999) 311.
13. M. H. HUANG, Y. WU, H. FEICK, N. TRAN, E. WEBER and P. YAMG, *Adv. Mater.* **13** (2001) 113.
14. Z. W. PAN, Z. R. DAI and Z. L. WANG, *Science* **291** (2001) 1947.
15. A. P. ALIVISATOS, *ibid.* **271** (1996) 993.
16. E. W. WONG, P. E. SHEEHAN and C. M. LIEBER, *ibid.* **277** (1997) 1971.
17. H. H. TIPPINS, *Phys. Rev.* **140** (1965) A316.
18. D. D. EDWARDS, T. O. MASON, F. GOUTENOIR and K. R. POPPELMEIER, *Appl. Phys. Lett.* **70** (1997) 1706.
19. L. BINET and D. GOURIER, *J. Phys. Chem. Solids* **59** (1998) 1241.
20. T. SHISHIDO *et al.*, unpublished (2004).
21. We consider the experimental error of about 10% by background subtraction and reduction due to electron beam irradiation in an ultra-high vacuum of TEM.
22. R. S. WAGNER and W. C. ELLIS, *Appl. Phys. Lett.* **4** (1964) 89.

Received 22 July  
and accepted 17 December 2004